Published in final edited form as:
Nucl Med Biol. 2007 April ; 34(3): 233–237.

Pharmacokinetics of [^{18}F]Fluoroalkyl Derivatives of Dihydrotetrabenazine (DTBZ) in Rat and Monkey Brain

Michael R. Kilbourn[1], **Brian Hockley**[1], **Lihsueh Lee**[1], **Catherine Hou**[2], **Rajesh Goswami**[2], **Datta E. Ponde**[2], **Mei-Ping Kung**[2], and **Hank F. Kung**[2]

1 *Department of Radiology, University of Michigan Medical School, Ann Arbor, MI*

2 *Department of Radiology, University of Pennsylvania, Philadelphia, PA*

Abstract

The specific binding and regional brain pharmacokinetics of new fluorine-18 labeled radioligands for the vesicular monoamine transporter (VMAT2) were examined in the rat and primate brain. In the rat, 9-[^{18}F]fluoropropyl-(±)-9-O-desmethyldihydrotetrabenazine ([^{18}F]FP-(±)-DTBZ) showed better specific binding in the striatum than either (+)-[^{11}C]dihydrotetrabenazine ([^{11}C]DTBZ) or 9-[^{18}F]fluoroethyl-(±)-9-O-desmethyldihydrotetrabenazine ([^{18}F]FE-(±)-DTBZ). Using microPET, the regional brain pharmacokinetics of [^{18}F]FE-(±)-DTBZ, [^{18}F]FP-(±)-DTBZ and (+)-[^{11}C]DTBZ were examined in the same monkey brain. (+)-[^{11}C]DTBZ and [^{18}F]FP-(±)-DTBZ showed similar brain uptakes and pharmacokinetics, with similar maximum striatum to cerebellum ratios (STR/CBL = 5.24 and 5.15, respectively) that were significantly better than obtained for [^{18}F]FE-(±)-DTBZ (STR/CBL = 2.55). Striatal distribution volume ratios calculated using Logan plot analysis confirmed the better specific binding for the fluoropropyl compound (DVR = 3.32) vs. the fluoroethyl compound (DVR = 2.37). Using the resolved single active isomer of the fluoropropyl compound, [^{18}F]FP-(+)-DTBZ, even better specific to non-specific distribution was obtained, yielding the highest distribution volume ratio (DVR = 6.2) yet obtained for a VMAT2 ligand in any species. The binding of [^{18}F]FP-(+)-DTBZ to the VMAT2 was shown to be reversible by administration of a competing dose of unlabeled tetrabenazine. Metabolic defluorination was slow and minor for the [^{18}F]fluoroalkylDTBZ ligands. The characteristics of high specific binding ratio, reversibility, metabolic stability, and longer half-life of the radionuclide make [^{18}F]FP-(+)-DTBZ a promising alternative VMAT2 radioligand suitable for widespread use in human PET studies of monoaminergic innervation of the brain.

Keywords

vesicular monoamine transporter; tomography; emission computed; tetrabenazine

1. Introduction

The imaging of the vesicular monoamine transporter (VMAT2) in the human brain using Posotron Emission Tomography (PET) and the radioligand (+)-[^{11}C]dihydrotetrabenazine ((+)-[^{11}C]DTBZ) has provided insights into the changes in numbers of dopaminergic synapses in a variety of neurological (Parkinson's, Alzheimer's, Tourette's, Huntington's, dystonia) and

CORRESPONDING AUTHOR ADDRESS: Michael R. Kilbourn, Ph.D., Cyclotron and Radiochemistry Facility, 2276, Medical Science I Building, University of Michigan, Ann Arbor. MI 48109, (734)763-9246, mkilbour@umich.edu

psychiatric (schizophrenia, bipolar disorder) diseases [1–8]. Most recently, the potential of PET imaging of [^{11}C]DTBZ binding in beta cells of the pancreas has been demonstrated [9, 10]. Widespread applications of VMAT2 imaging are however limited by the necessity for an on-site medical cyclotron and associated radiochemical expertise for the synthesis of the carbon-11 ($t_{1/2}$ = 20.4 min) labeled radiopharmaceutical. Increased use of VMAT2 imaging would be greatly facilitated by availability of ligands with longer half-lives, such that the radiopharmaceutical might be regionally produced and distributed to sites not possessing cyclotron facilities. To that end, we have recently reported the synthesis and initial evaluation of fluorine-18 ($t_{1/2}$ = 110 min) derivatives of DTBZ. Two derivatives, 9-[^{18}F]fluoroethyl-(±)-9-O- desmethyldihydrotetrabenazine (FE-(±)-DTBZ) and 9-[^{18}F]fluoropropyl-(±)-9-O-desmethyldihydrotetrabenazine (FP-(±)-DTBZ) (Fig. 1) emerged as high affinity (K_i = 0.76 and 0.56 nM, respectively) radioligands which demonstrated excellent in vivo properties of high brain uptake and a regional distribution of saturable binding consistent with the distribution of the VMAT2 in monoaminergic terminals [11].

As the next step in development of one of these fluorinated radioligands for human use, they were examined here for distribution and pharmacokinetics in the rat and monkey brain. In particular FE-(±)-DTBZ , FP-(±)-DTBZ, and the recently resolved higher affinity isomer FP-(+)-DTBZ [12] were directly compared with (+)-[^{11}C]DTBZ in the primate brain.

2. Materials and Methods

2.1. Radiochemical syntheses

Syntheses of the mesylate precursors to FE-(±)-DTBZ and FP-(±)-DTBZ have been previously reported [11]. Synthesis of the mesylate precursor to the optically active isomer FP-(+)-DTBZ was done in an analogous fashion [12] starting with the resolved (+)-9-O-desmethylDTBZ ((+)-(2R,3R,11bR)-9-O-desmethyldihydrotetrabenazine) obtained form the NIMH Chemical Synthesis and Drug Supply Program.

Fluorine-18 was produced on the University of Michigan CS-30 cyclotron and prepared for reaction by azeotropic distillation of water using acetonitrile. [^{18}F]Fluoride ion was resolubolized using potassium carbonate/Kryptofix and reacted with the mesylate precursors using minor modifications of the procedure of Goswami et al [11]. Radiochemical products were isolated and purified using HPLC. Yields were 5 –10% corrected for decay in a synthesis time of 60 min, with specific activities of 410 ± 57 Ci/mmol; no efforts were made to optimize either radiochemical yields or specific activities for these experiments.

2.2. Animals

Rat studies were done using 200–300 g Sprague-Dawley rats (Charles Rivers, Portage, MI). Primate studies were done in young mature female rhesus monkeys. All animal studies were approved by the University of Michigan Committee on Use and Care of Animals.

2.3. Rat brain biodistributions

Regional rat brain biodistributions were done using the bolus plus constant infusion protocol previously developed for studies with [^{11}C/^{3}H]DTBZ [13,14]. In brief, animals were lightly anesthetized with diethyl ether, a tail vein catheter inserted, and the animals placed in restraint tubes and allowed to awaken. Radiotracers (50 ± 3 microcuries in 1.5 ml isotonic saline) were then given as a bolus (1 ml) in 1 minute followed by constant infusion of 0.5 ml over the remaining 59 minutes. At the end of one hour the animals were killed by intravenous injection of a sodium barbituate overdose, and the brain rapidly excised and dissected into regions of interest. Tissue samples were weighed and counted for fluorine-18. Data was calculated as

percent injected dose/g tissue and as tissue distribution volume ratios (DVR) relative to the cerebellum.

2.4. Primate microPET imaging

Imaging of monkey brains was done using the Concorde Microsystems P4 tomograph. Animals were anesthetized (isoflurane), intubated, a venous catheter inserted into one hindlimb, and the animal positioned on the bed of the MicroPET gantry. Isoflurane anesthesia was continued throughout the study. After completion of the transmission scan, animals were injected with radiochemical (1.04 – 5.85 mCi in 1–3 mL isotonic saline) as a bolus over 1 minute. Emission data was collected for 60 or 90 minutes. For a dual $^{11}C/^{18}F$ study session, the second radiochemical (a fluorine-18 labeled tracer) was injected one hour after the end of the [^{11}C]DTBZ imaging period, and a second emission scan collected for 60 minutes. For the unlabeled TBZ displacement study, TBZ (2 mg/kg in saline) was injected intravenously at 40 minutes after the start of the scan.

Emission data was corrected for attenuation and scatter and reconstructed using the 3-D maximum a priori method (3-D MAP algorithm). Using a late image, regions of interest were drawn manually on multiple planes to obtain volumetric ROIs for the striatum and where possible other regions of intermediate VMAT2 density (thalamus, raphe). Using a summed image of early frames, where radiotracer distribution was mostly blood flow delivery, the cerebellum and cortex were readily identified and a regions of interest drawn on multiple planes. The volumetric regions of interests were then applied to the full dynamic data set to obtain the regional tissue time-radioactivity data. Radioactivity concentrations (nCi/cc) were normalized to injected doses of radiotracers, and striatal distribution volume ratios (DVR) calculated using the cerebellum to represent the non-specific binding region in a Logan plot analysis [15].

3. Results

The 9-[^{18}F]fluoroalkyl derivatives of dihydrotetrabenazine were developed as alternatives to carbon-11 labeled derivatives of dihydrotetrabenazine[16] which have been used as successful ligands for the imaging of the vesicular monoamine transporter type 2 (VMAT2) in the human brain [17]. The fluoroethyl and fluoropropyl derivatives have high in vitro binding affinities for the VMAT2 site, and showed specific binding in mouse brain both in vitro and in vivo [11].

Evaluation of the racemic forms of the two fluorinated ligands in the awake rat brain, using a quantitative equilibrium distribution technique previously developed [13,14], showed regional brain distributions of specific radioligand binding entirely consistent with the tissue concentrations of the VMAT2 determined from in vitro assays, with highest specific binding in the striatum, intermediate in the hypothalamus, and lowest in the cerebellum (Table 1). The regional distributions of specific binding for both [^{18}F]fluoroalkylDTBZ derivatives also correlate highly with the distribution of in vivo binding of [^{3}H]DTBZ ($r^2 = 0.98$ for both, data not shown). As was previously observed in the mouse [11], the racemic [^{18}F]fluoropropyl compound shows better specific binding in the rat striatum (DVR = 4.54 ± 0.31) than the resolved (+)-DTBZ (DVR = 3.62 ± 0.33); the lowest brain uptake and poorest specific binding in striatum are observed for the racemic [^{18}F]fluoroethyl derivative (DVR = 2.91 ± 0.07).

These results in rats were highly encouraging and matched the previous observations in mice, but they did not answer the crucial questions regarding brain uptake and pharmacokinetics in the primate brain, or the possibility of rapid metabolic defluorination (to produce [^{18}F]fluoride ion) which might occur in higher species. To answer these questions the pharmacokinetics of (+)-[^{11}C]DTBZ, [^{18}F]FE-(±)-DTBZ, and [^{18}F]FP-(±)-DTBZ were examined in the same

monkey brain. The study design combined a 60 minute [^{11}C]DTBZ imaging study, a one hour interval, followed by a one hour imaging with one of the fluorinated radioligands. Representative late images for each of the three radioligands are shown in Fig. 2, and the tissue time-activity curves normalized for injected dose are shown in Fig. 3. Using the brain penetration (as evidenced by maximal concentrations in striatum) and simple striatum to cerebellum ratios (Table 2) as the first indicators of differences between the radioligands, [^{18}F]FP-(±)-DTBZ and (+)-[^{11}C]DTBZ were very similar, and both significantly better than [^{18}F]FE-(±)-DTBZ. The distinctions between the radioligands are entirely in striatal uptake and retention, as the cerebellar concentrations (representing non-specific distributions) are essentially identical for all three at later time points. Metabolic defluorination and uptake of [^{18}F]fluoride ion into the skull of the animal was slow and quite low compared to radioligand accumulation in the basal ganglia. For every study uptake in the region of the eye was observed: although even [^{11}C]DTBZ shows such in primates due to the presence of VMAT2 [18] it does not do so in the human. The tissue time-radioactivity data were then analyzed using a Logan plot to provide estimates of the distribution volume ratios (DVR) for all three radioligands (Table 2). Consistent with both the mouse and rat studies completed earlier, the in vivo uptake and regional distribution of [^{18}F]FP-(±)-DTBZ was significantly better than that of [^{18}F]FE-(±)-DTBZ, and the [^{18}F]fluoropropyl compound was thus chosen for further evaluation in the monkey model.

As resolution of the stereoisomers of racemic dihydrotetrabenazine [19] had provided a higher affinity ligand in the form of the single (+)-DTBZ isomer [20] subsequent studies were done with [^{18}F]FP-(+)-DTBZ; the necessary mesylate precursor for this chiral radioligand was readily prepared from the same precursor (9-O-desmethylDTBZ) used for (+)-[^{11}C]DTBZ [12]. Consistent with the observations in animal and human studies [15] upon moving from racemic to resolved [^{11}C]DTBZ, the inactive (−)-isomer of the fluoropropyl compound also has very low binding affinity (K_i > 3000 nM) relative to the active (+)-isomer (K_i = 0.10 nM) [12], and the PET imaging study of [^{18}F]FP-(+)-DTBZ showed the expected improvement of the distribution of specific vs. nonspecific binding (Fig. 1), with higher striatum to cerebellum ratios (maximum of 5.6 at 90 min), resulting in a DVR value of >6 for this chiral fluorinated ligand. These are the highest values yet obtained for a VMAT2 radioligand in vivo in any species. The improved signal-to-noise for this radioligand also permitted easier identification of other structures, such as the thalamus and a region assigned as perhaps the raphe, known to have intermediate levels of monoaminergic neuronal innervation.

The final study was done to demonstrate that binding of [^{18}F]FP-(+)-DTBZ to the VMAT2 in the primate brain was reversible and could be competed for by a large dose of cold tetrabenazine. Administration of tetrabenazine 40 minutes after injection of [^{18}F]FP-(+)-DTBZ produced a rapid loss of radioactivity in the striatum, as well as in thalamus and raphe, but no change in the cerebellar or cortical concentration (Fig. 4). The striatum to cerebellum ratio was significantly reduced by 45% at 90 minutes and was continuing to decrease at the end of the study.

4. Discussion

These studies of pharmacokinetics in the primate brain, together with the in vitro and in vivo results obtained in mouse and rat brain, support that [^{18}F]FP-(+)-DTBZ should be an excellent in vivo radioligand for imaging of the VMAT2 in the brain. In both rodent and primate, brain penetration and ratios of specific to nonspecific binding are better than with the carbon-11 radioligand currently in human and animal use for PET imaging. Metabolism to lose [^{18}F] fluoride ion, always a potential concern with fluorine-18 labeled ligands, does not appear to be a significant problem. Further studies in rodent and primate brain with this promising radioligand are in progress and will be reported in the near future.

Acknowledgements

This work was supported by grants awarded from the National Institutes of Health (NS-015655 for M.R. K. and EB-002171 for H.F. K.). We are grateful to the National Institute of Mental Health's Chemical Synthesis and Drug Supply Program for providing the samples of resolved (+)-9-O-desmethyl-DTBZ used in this work, and thank Dr. Robert Koeppe for Logan plot pharmacokinetic analyses.

References

1. Albin RL, Koeppe RA, Bohnen NI, Nichols TE, Meyer P, Wernette K, Minoshima S, Kilbourn MR, Frey K. Increased ventral striatal monoaminergic innervation in Tourette syndrome. Neurology 2003;61:310–5. [PubMed: 12913189]
2. Bohnen NI, Albin RL, Koeppe RA, Wernette KA, Kilbourn MR, Minoshima S, Frey KA. Positron emission tomography of monoaminergic vesicular binding in aging and Parkinson disease. J Cerebral Blood Flow Metab 2006;26:1198–212.
3. Bohnen NI, Koeppe RA, Meyer P, Ficaro E, Wernette K, Kilbourn MR, Kuhl DE, Frey KA, Albin RL. Decreased striatal monoaminergic terminals in Huntington disease. Neurology 2000;54:1753–9. [PubMed: 10802780]
4. De La Fuente-Fernandez R, Furtado S, Guttman M, Furukawa Y, Lee CS, Calne DB, Ruth TJ, Stoessl AJ. VMAT2 binding is elevated in dopa-responsive dystonia: visualizing empty vesicles by PET. Synapse 2003;49:20–8. [PubMed: 12710012]
5. Gilman S, Koeppe RA, Chervin RD, Consens FB, Little R, An H, Junck L, Heumann M. REM sleep behavior disorder is related to striatal monoaminergic deficit in MSA. Neurology 2003;61:29–3. [PubMed: 12847152]
6. Gilman S, Koeppe RA, Little R, An H, Junck L, Giordani B, Persad C, Heumann M, Wernette K. Striatal monoamine terminals in Lewy body dementia and Alzheimer's disease. Ann Neurol 2004;55:774–80. [PubMed: 15174011]
7. Koeppe RA, Gilman S, Joshi A, Liu S, Little R, Junck L, Heumann M, Frey KA, Albin RL. ^{11}C-DTBZ and ^{18}F-FDG PET measures in differentiating dementias. J Nucl Med 2005;46:936–44. [PubMed: 15937303]
8. Zubieta JK, Taylor SF, Huguelet P, Koeppe RA, Kilbourn MR, Frey KA. Vesicular monoamine transporter concentrations in bipolar disorder type I, schizophrenia, and healthy subjects. Biol Psych 2001;49:110–6.
9. Simpson NR, Souza F, Witkowski P, Maffei A, Raffo A, Herron A, Kilbourn M, Jurewicz A, Herold K, Liu E, Hardy MA, Van Heertum R, Harris PE. Visualizing pancreatic beta-cell mass with [^{11}C] DTBZ. Nucl Med Biol 2006;33:855–6. [PubMed: 17045165]
10. Souza F, Simpson N, Raffo A, Saxena C, Maffei A, Hardy M, Kilbourn M, Goland R, Leibel R, Mann JJ, Van Heertum R, Harris PE. Longitudinal noninvasive PET-based beta cell mass estimates in a spontaneous diabetes rat model. J Clin Invest 2006;116:1506–13. [PubMed: 16710474]
11. Goswami R, Kung M-P, Ponde D, Hou C, Kilbourn MR, Kung HF. Fluoroalkyl derivatives of dihydrotetrabenazine as PET imaging agents targeting vesicular monoamine transporters. Nuc Med Biol 2006;33:685–694.
12. Kung M-P, Hou C, Goswami R, Ponde DE, Kilbourn MR, Kung HF. Characterization of optically resolved 9-fluoropropyl-dihydrotetrabenazine as a potential PET imaging agent targeting vesicular monoamine transporters. submitted to Nuclear Medicine and Biology
13. Kilbourn MR, Sherman PS, Kuszpit K. In vivo measures of dopaminergic radioligands in the rat brain: equilibrium infusion studies. Synapse 2002;43:188–94. [PubMed: 11793424]
14. Kilbourn MR. Long-term reproducibility of in vivo measures of specific binding of radioligands in rat brain. Nucl Med Biol 2004;31:591–5. [PubMed: 15219277]
15. Koeppe RA, Frey KA, Kuhl DE, Kilbourn MR. Assessment of extrastriatal vesicular monoamine transporter binding site density using stereoisomers of [^{11}C]dihydrotetrabenazine. J Cerebral Blood Flow Metab 1999;9:1376–84.
16. Kilbourn MR. In vivo radiotracers for vesicular neurotransmitter transporters. Nucl Med Biol 1997;24:615–619. [PubMed: 9352531]

17. Frey KA, Koeppe RA, Kilbourn MR. Imaging the vesicular monoamine transporter. Adv Neurol 2001;86:237–47. [PubMed: 11553983]

18. Lutjen-Drecoll E. Choroidal innervation in primate eye. Exp Eye Res 2006;82:357–6. [PubMed: 16289045]

19. Kilbourn MR, Lee LC, Jewett DM, Heeg MJ. The absolute configuration of (+)-α-dihydrotetrabenazine, an active metabolite of tetrabenazine. Chirality 1997;9:59–62. [PubMed: 9094204]

20. Kilbourn MR, Lee L, Vander Borght T, Jewett D, Frey K. Binding of α-dihydrotetrabenazine to the vesicular monoamine transporter is stereospecific. Eur J Pharmacol 1995;278:249–252. [PubMed: 7589162]

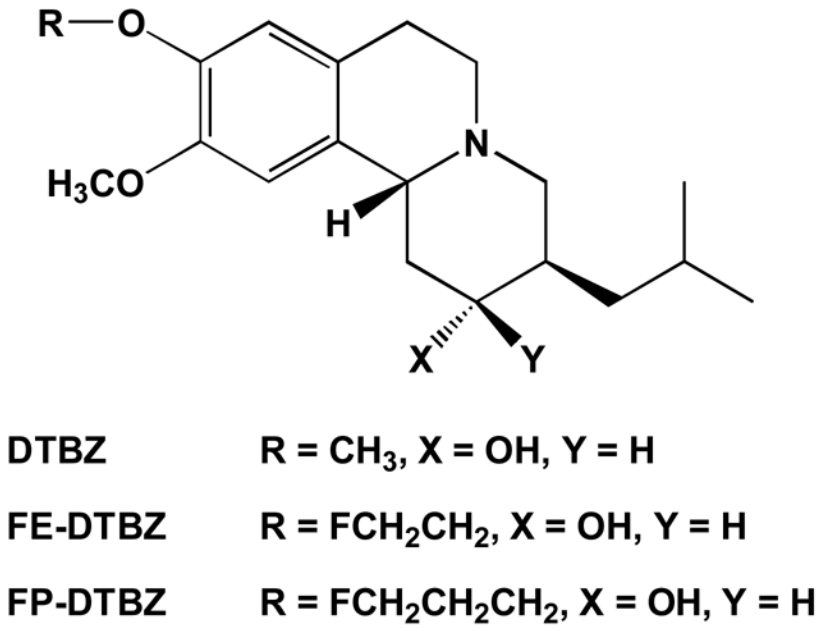

Figure 1.
Structures of VMAT2 radioligands

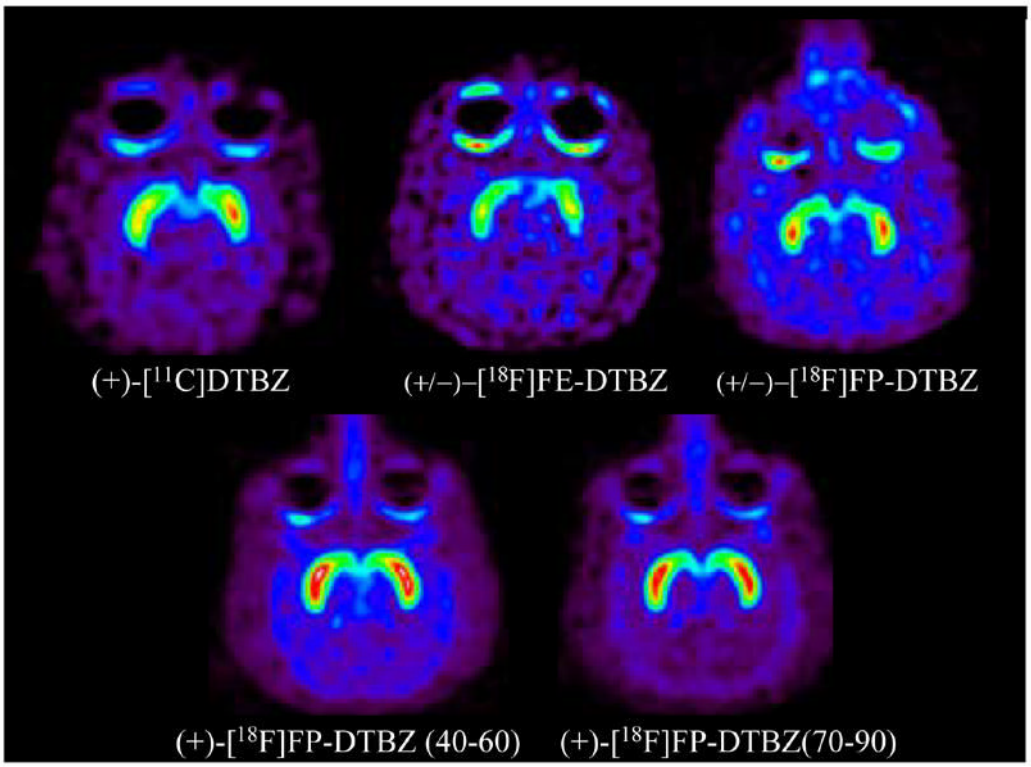

Fig 2.

Monkey microPET images (+)-[^{11}C]dihydrotetrabenazine (DTBZ), (±)-[^{18}F]fluoroethyldihydrotetrabenazine (FE-DTBZ), (±)-[^{18}F]fluoropropyldihydrotetrabenazine (FP-DTBZ), and (+)-[^{18}F]fluoropropylDTBZ. Images are transaxial slices at the level of the striatum, representing summations of the last 20 minutes of emission data (40–60 min for (+)-DTBZ, (±)-FE-DTBZ, and (±)-FP-DTBZ).

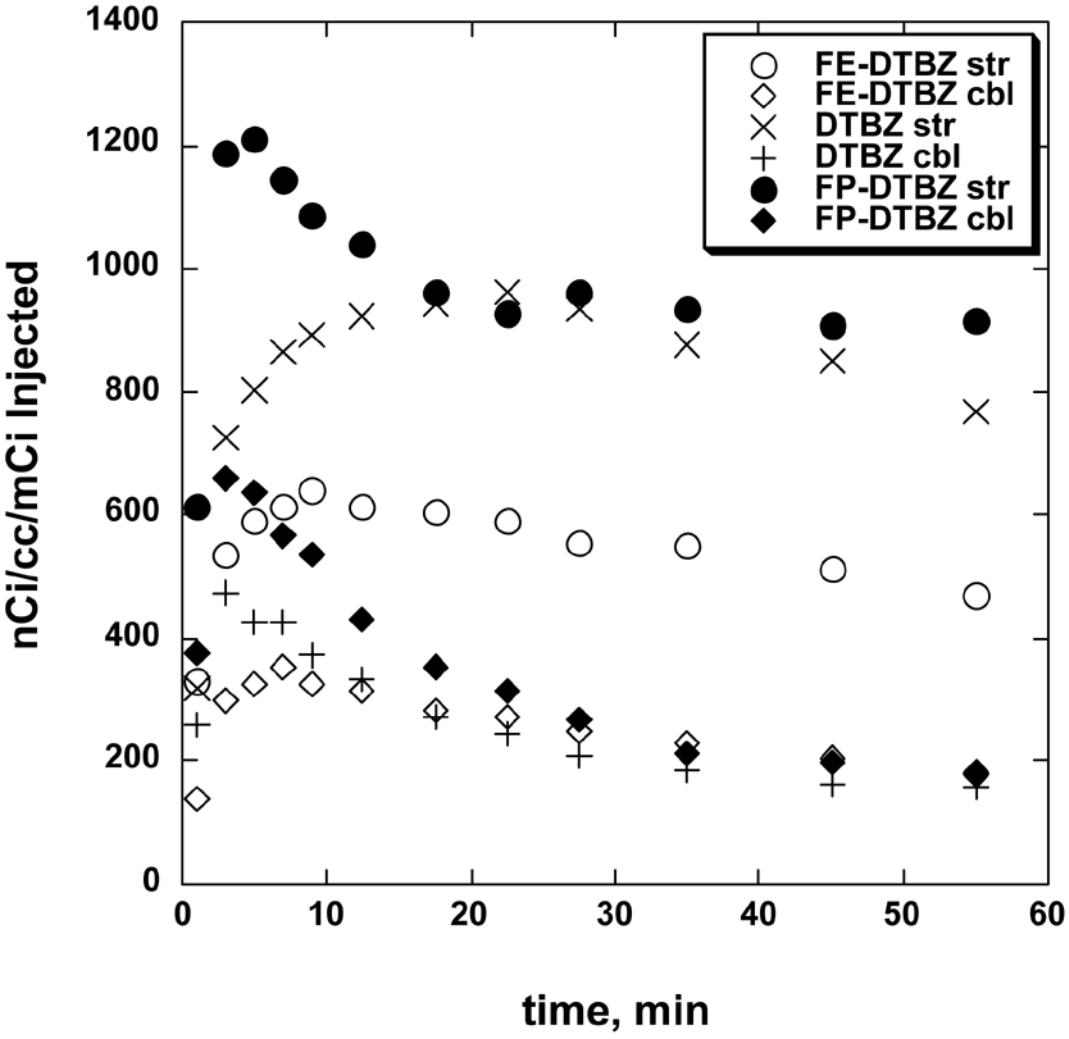

Fig 3.

Tissue time vs. radioactivity curves for striatum and cerebellum regions of interest for (+)-[^{11}C]DTBZ, [^{18}F]FE-(±)-DTBZ, and [^{18}F]FP-(±)-DTBZ in rhesus monkey brain (same animal for all studies).

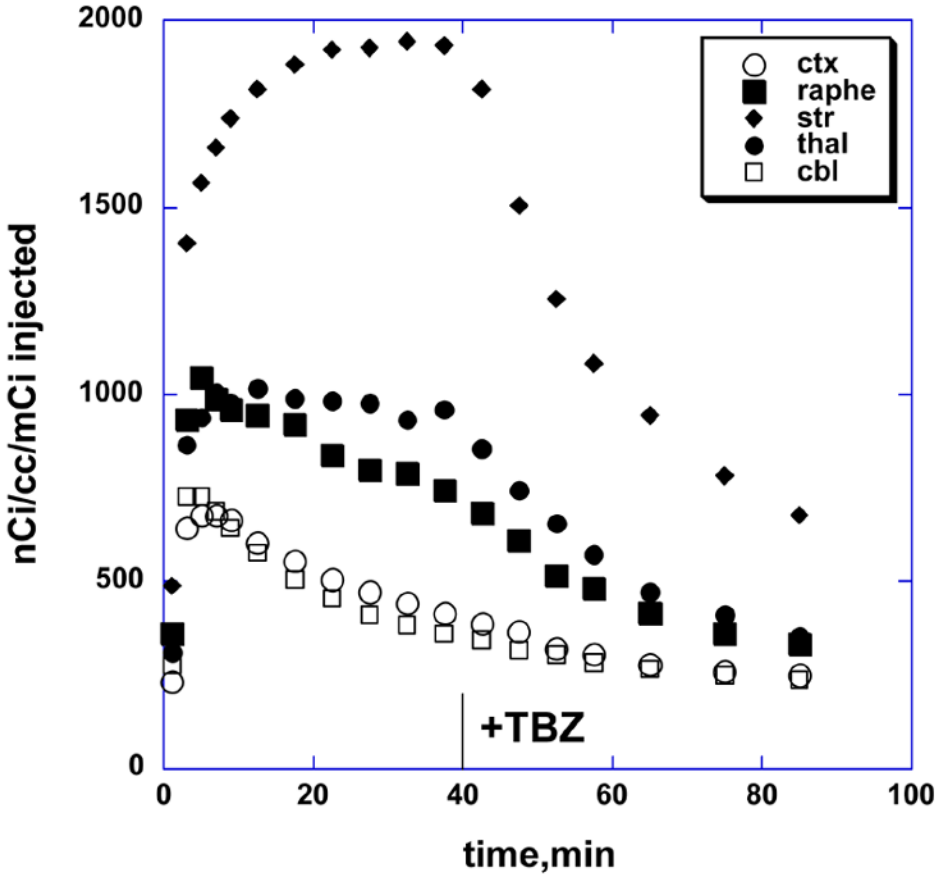

Fig 4.

Tissue time vs. radioactivity curves for striatum, cortex, raphe, thalamus and cerebellum regions of interest for [^{18}F]FP-(±)-DTBZ in rhesus monkey brain, with intravenous injection of 2 mg/kg tetrabenazine at 40 minutes.

Table 1

Regional distribution of specific binding (distribution volume ratios (DVR) relative to cerebellum) for (±)-[^{18}F] fluoroethylDTBZ (FE-DTBZ), (±)-[^{18}F]fluoropropylDTBZ (FP-DTBZ), and (+)-[^{11}C]DTBZ in the rat brain. Data are mean ± standard deviation with N = 4 for each FE- and FP-DTBZ, and N = 35 for DTBZ. Data for [^{11}C]DTBZ from reference [14]. nd = not determined.

	FE-DTBZ	FP-DTBZ	C-11 DTBZ
striatum	2.91 ± 0.07	4.54 ± 0.31	3.62 ± 0.33
cortex	1.25 ± 0.03	1.36 ± 0.02	nd
hippocampus	1.21 ± 0.07	1.38 ± 0.19	nd
hypothalamus	1.70 ± 0.04	2.93 ± 0.27	2.20 ± 0.34
thalamus	1.33 ± 0.04	1.68 ± 0.18	nd

Table 2

Maximum striatum to cerebellum ratios and calculated distribution volume ratios (DVR relative to cerebellum) for VMAT2 radioligands in rhesus monkey brain. All studies done in the same monkey. DVR values obtained by Logan plot analysis.

	STR/CBL	Striatal DVR
(+)-[^{11}C]DTBZ	5.24	4.54
(±)-[^{18}F]FE-DTBZ	2.55	2.37
(±)-[^{18}F]FP-DTBZ	5.15	3.32
(+)-[^{18}F]FP-DTBZ	5.60	6.2